Astron. Astrophys. 345, 430–438 (1999)

ASTRONOMY AND ASTROPHYSICS

Abundances of cool supergiants in the SMC young cluster NGC 330*

V. Hill[1,2]

[1] ESO, Karl-Schwarschild-Strasse 2, D-85748 Garching bei München, Germany (vhill@eso.org)
[2] DASGAL, UMR 8633 du CNRS, Observatoire de Meudon, F-92195 Meudon CEDEX, France

Received 23 December 1998 / Accepted 16 February 1999

Abstract. NGC 330 is the brightest SMC young cluster and contains many bright supergiants. This cluster has aroused special interest, since the earlier abundance determinations indicated an abundance lower by a factor ∼5 than in the SMC field young population. Taking advantage of our previous high resolution analysis of a sample of type K supergiants in the SMC field (Paper I and II), we analyse 6 cool supergiants in NGC 330, in order to compare in an homogeneous way, the metallicity and abundance ratios of various elements in NGC 330 and in the field of the SMC. The main results may be summarised as follows:

• the deficiency of NGC 330 is found to be of [Fe/H] = -0.82 ± 0.11 dex (mean and rms for 6 stars) whereas the field stars had a [Fe/H] = -0.69 ± 0.10 dex (mean and rms for 6 stars). A slight difference may exist between the field and the cluster stars, but this difference is small.
• the abundance pattern of the ∼20 elements studied, is similar to that of the field supergiants, except for a few elements: oxygen's star to star scatter is significantly larger in the cluster; the very heavy neutron capture process elements are less enhanced in the cluster.
• lithium is detected in five stars and is low, indicating that the stars underwent dilution (mean value and rms for the 5 stars: log $\epsilon(Li) \simeq 0.1 \pm 0.2$ dex).

Key words: stars: abundances – stars: supergiants – galaxies: abundances – galaxies: Magellanic Clouds

1. Introduction

NGC 330 is the brightest of the SMC young clusters, and contains many bright red and blue supergiants (the age of NGC 330 is around 20–25 Myrs). This cluster has aroused special interest, since the earlier abundance determination (from photometry: Carney et al. 1985; from spectroscopy: Spite et al. 1986) indicated an abundance much lower (by a factor 5). than the young field population of the SMC. How could a young cluster form with a metallicity lower than that of the surrounding field?

Moreover, the young population in the field of the SMC seems to be fairly well mixed: no abundance gradient nor large scatter are found among the K supergiants (Paper I), nor among the H II regions (Russell & Dopita 1990 and references therein). Since then, the strong metal-deficiency of NGC 330 has been questioned:

The value of the reddening, initially found to be small (E(B-V)=0.03 Carney et al. 1985) was challenged by Bessell (1991) who suggested a higher value of E(B-V)=0.12, which would increase the adopted effective temperatures of the stars studied by spectroscopy, and in turn, increase the abundance deduced.

However, Spite et al. (1991) analysed four supergiants in NGC 330 (two F type and two K type) and showed that the temperatures deduced from the (B-V) colors corrected with such a high value of the reddening were incompatible with other temperature indicators (excitation equilibrium, Hα profiles). They finally came out with an abundance of [Fe/H] = -1.0 ± 0.1 dex for these stars (a factor 2.5 below the SMC field stars).

Strömgren photometry of supergiants in NGC 330 (Grebel & Richtler 1992) suggested an over-deficiency of the cluster by a factor 3 compared to the surrounding field ([M/H] = -1.26 and -0.76 respectively) whereas a more recent work by Hilker et al. (1994) suggested a somewhat milder deficiency of [M/H] = -0.93 ± -0.16 dex.

On the other hand, Meliani et al. (1995) analysed five type K supergiants by medium resolution spectroscopy and found a mean metallicity of [M/H] = -0.67 dex. From the same kind of analysis, Jasniewicz & Thévenin (1994) found no overdeficency of NGC 330 versus field supergiants.

The question of the metallicity of NGC 330 (relative to its surrounding field) is thus still open. The aim of this work is to compare in the most homogeneous way, the abundances of NGC 330 and of the young stars in the field of the SMC. Taking advantage of our previous high resolution analysis of a sample of type K supergiants in the field of the SMC (Hill 1997 Paper I, and Hill et al. 1997 Paper II), we analyse six K type supergiants in NGC 330 (four new ones and two that were already analysed by Spite et al. 1991) in the same way as the field supergiants and investigate both the overall metallicity and the abundance ratios of various elements. The abundances of 16 elements from sodium to europium are derived and discussed.

Send offprint requests to: V. Hill

* Based on observations collected at the European Southern Observatory, La Silla, Chile.

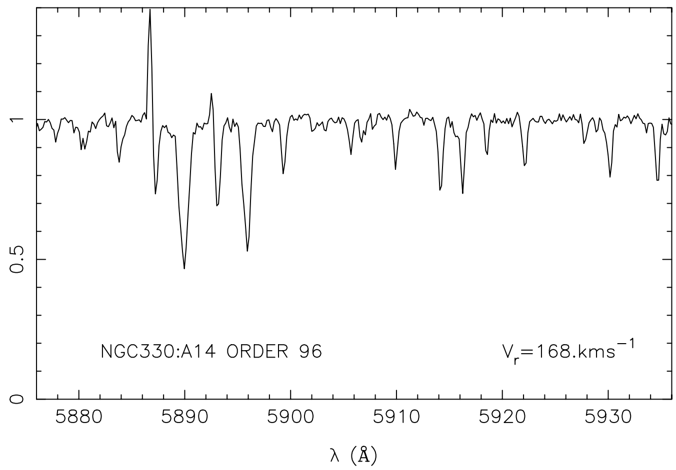

Fig. 1. Example of a reduced portion of the a spectrum: order number 96 of the echelle spectrum of NGC30:A 14. One can see the Na I doublet of the star at 5889 and 5892 Å, and blueward, the interstellar absorption and the emission of the night sky.

2. Observations

In addition to the two cool supergiants (A7, B40) already published by Spite et al. 1991, we observed four new G to K supergiants (A3, A6, A14 and A45).The identifications of the stars are from Robertson (1974). These observations were carried out in 1990 and 1991 on CASPEC fed by the 3.6m telescope at ESO, La Silla. A brief logbook of the these observations together with the older ones is given Table 1.

Our final sample consists of six supergiant stars, selected from Robertson 1974 on the basis of their probability to belong to the cluster and the feasability of the observation (bright enough and not too close to the center, avoiding severe crowding effects). The magnitude and colours of the stars can be found in Table 2.

The spectra have a resolving power of R≈20000, and the signal to noise ratios are of S/N=80 to 100 on average. For each star, we obtained two overlapping échelle spectra in order to cover a large spectral range, and the overlapping region was used to reduce the stochastic errors on the equivalent width of the spectral lines by averaging the measurements from the two spectra.

The spectra were reduced using a semi-automatic code especially developed by Spite(1990) which finds and extracts the spectral orders (optimal extraction), performs flat fielding and wavelength calibration from the comparison lamp spectrum and computes the radial velocity. An example of a reduced spectrum is given in Fig. 1

3. Analysis

In order to compare in the most homogeneous fashion the chemical compositions of the NGC 330 stars and the field SMC stars, we followed closely as the analysis used to derive the abundances of the SMC field stars (Paper I). Details can be found in

Table 1. Logbook of the observations

star	Date	Instrument	$\Delta\lambda(nm)$	V_r (kms^{-1})
A 3	Oct 91	CASPEC	460–610	155.4
A 3	Oct 91	CASPEC	530–700	155.1
A 6	Dec 90	CASPEC	455–600	154.1
A 6	Dec 90	CASPEC	540–685	154.1
A 7*	*Dec 89*	*CASPEC*	*510–600*	*155.2*
A 7*	*Oct 85*	*CASPEC*	*590–680*	*154.7*
A 14	Oct 91	CASPEC	460–610	159.8
A 14	Oct 91	CASPEC	530–700	156.3
A 45	Oct 91	CASPEC	460–610	155.5
A 45	Oct 91	CASPEC	530–700	155.6
B 40*	*Dec 89*	*CASPEC*	*590–680*	*152.1*

* these are the spectra that were used in Spite et al. 1991

Sect. 3 of Paper I. Let us here briefly remind the main characteristics of the analysis:

3.1. Stellar atmosphere models

The model atmospheres that we used to derive the abundances were interpolated in grids of models calculated with codes derived from the MARCS', and specially adapted to represent the atmosphere of low gravity stars: Plez's (1995 and 1997) grid of models, with temperature and gravity ranges (3500≤$T_{\rm eff}$ ≤4750 K and −0.5≤log g≤1.0 dex) for metallicities −1.0, −0.6, −0.3, 0., 0.3, 0.6 dex.

3.2. Effective parameter determination

To remain as homogeneous as possible with our previous analysis of SMC field stars (Paper I), we used the same procedure to determine the effective parameters of the stars that is:

Temperature: after a first guess from the colours of the star, $T_{\rm eff}$ is determined "spectroscopically" so that the excitation equilibrium is achieved, asking that lines with high and low excitation potential should produce the same abundance for a given element (here Fe I). (See below for a comparison of the Teff indicators used and their sources.)

Surface gravity: log $g$is derived from the ionisation equilibrium: we require that the iron abundance deduced from neutral and ionised species should be the same.

Microturbulent velocity: v_t is derived asking that the iron lines with small and large equivalent widths should give the same abundance.

3.2.1. Photometry

The $(B-V)$ colour indice is known to be a poor temperature indicator for cool supergiants (gravity dependent). In order to have a better hold on the effective temperature of the stars under study, we decided to acquire photometry for this cluster, in particular, $(V-I)$ colours which are well correlated to the effective temperature for cool supergiants (e.g. Bessell et al. 1998).

Table 2. Photometry and temperatures for the program stars

star	V	$(B-V)$	$(V-R)$	$(V-I)$	Temperatures (in K) deduced from: $(V-I)$ using $E(B-V)$= 0.03	0.09	0.12	$(V-K)^*$ 0.12	**spectroscopy**	Notes
A 3	13.90	1.17	0.56	1.12	4650	4900	5000	*5100*	**4800**	
A 6	13.57	1.66	0.82	1.52	4100	4250	4300	*4200*	**4250**	
A 7				*1.72*	3800	3950	4000	*4050*	**4000**	1
A 14	13.67	1.70	0.87	1.64	3900	4050	4100	*4150*	**4100**	
A 45	13.68	0.96	0.55	1.15	4600	4850	5000		**4400**	2
B 40	13.41	1.62	0.78	1.48	4100	4200	4350	*4300*	**4300**	

* The temperatures deduced from the $(V-K)$ color indices were kindly provided by M. Bessell, since we did not observe in the K band.

1: A7 (V=13) was saturated on our R and I exposures. The $(V-I)$ color is from Bessell.

2: A45 is situated at the very center of the cluster, and has bright neighbours which contaminate its photometry

E. Maurice kindly lent us his BVRI CCD data on NGC 330 (taken in December 1993 at the Danish 1.54m telescope in ESO La Silla). The images were processed with the classical procedures: substracting bias, dividing by a flat-field (mean of 10 dome flat-field). The photometry of the stars was then extracted using DAOPHOT PSF-fitting routines. Sequences of standard stars were also observed: Vigneau & Azzopardi (1982) SMC standard sequence as primary standards and Alcaino & Alvarado (1988) NGC 330 photoelectric sequence as secondary standards. The residual dispersions (σ) around the photometric standard sequence are: $\sigma_V = 0.021$ $\sigma_{(B-V)} = 0.024$ $\sigma_{(V-R)} = 0.012$ and $\sigma_{(V-I)} = 0.006$.

Table 2 gives the derived V magnitude and $(B-V)$, $(V-R)$ and $(V-I)$ colours for the stars in our sample.

3.2.2. Comparison of various temperature indicators

Also tabulated in Table 2 are the effective temperatures $T_{\rm eff}$ derived for each of the stars, using various indicators:

$(V-I)$ *colour:* $T_{\rm eff}$ is deduced from the confrontation of the observed $(V-I)$ colour (our own CCD photometry) with the ones calculated from Plez' model, with reddening values of $E(B-V)$ =0.03, 0.12 and 0.09, corresponding respectively to the values recommended by Carney et al. (1985), Bessell (1991) and Caloi et al. (1993), the latter being the most recent determination.

$(V-K)$ *colour:* $T_{\rm eff}$ is deduced from the confrontation of the observed $(V-K)$ colour (Bessell 1995) with the ones calculated from Plez' model, with a reddening of $E(B-V) = 0.12$.

"spectroscopic"determination: based on the excitation equilibrium, asking that high and low excitation potential lines of a given species (namely iron) yield the same abundance (there should be no trend of the resulting abundance with the excitation potential of the lines). *This determination is independent of reddening.*

The very close agreement between both (V-I) and (V-K) colour indices (when the most recent determination for the reddening $E(B-V) = 0.09$ is adopted) and the spectroscopic temperature indicator is striking. The concordance of independent ("photometric" and "spectroscopic") indicators is very encouraging, and allows us to rely on our temperature determinations. Moreover, the low value of $E(B-V) = 0.03$ for the reddening, seems to be ruled out. Table 3 summarises the final adopted effective parameters for each of the program star.

Table 3. Adopted effective parameters

Star	$T_{\rm eff}$ (K)	log $g(dex)$	v_t (kms^{-1})
A3	4800	0.5	3.
A6	4250	0.0	3.
A7	4000	-0.3	3.
A14	4100	-0.4	3.
A45	4400	-0.1	2.3
B40	4300	0.2	3.

For the two stars that were analysed by Spite et al. 1991, the adopted effective parameters are consistent within the expected uncertainty (the difference in $T_{\rm eff}$ is respectively +100 and +200 K, -0.1 and -0.2 dex in log *g*and -0.6–0.2 in v_t). The overall effect on the iron abundance determination (Spite et al. 1991 derive [Fe/H]= -1.05 and -0.95 dex respectively for A7 and B40, whereas we obtained -0.72 and -0.76 dex) comes mostly from the adopted higher effective temperatures, for which we are now confident, as we showed in the previous paragraph. The microturlulence velocity also plays a role here: we systematically adopted a somwhat lower v_t , which is a direct consequence our choice to restrict the study to relatively faint lines (see Sect. 3.3).

3.3. Atomic lines

For the abundance analysis, we chose to restrict ourselves to the relatively weak lines: below the saturation of the curve of growth (which corresponds to equivalents widths of the order of 200 mÅ) the abundances deduced from the lines are very little dependent upon the microturbulent velocity (v_t). Since

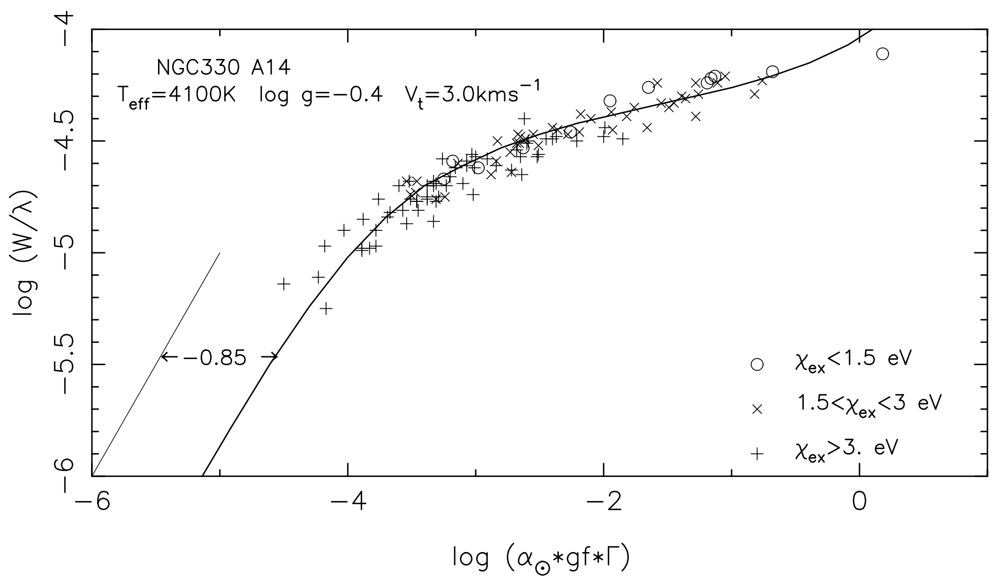

Fig. 2. Empirical and theoretical curves of growth of Fe I for the star NGC 330:A 14. The abscissa is $X = \log\alpha_{\odot} + \log gf + \log\Gamma(T_{eff}, g, M)$, where $\alpha_{\odot}$ is the abundance of the element in the Sun, gf the line transition probability and Γ (Cayrel & Jugaku, 1963) a function of the element M and of the stellar model. The horizontal distance between the thin line (defined by $W/\lambda = X$) and the solid line (theoretical curve of growth) gives directly [Fe/H] = −0.85 dex.

this parameter is not very well known in these stars, we only took into account the abundances calculated from lines with W $\leq$ 200 mÅ. For most lines, we determined equivalent widths by the Gaussian approximation and deduced the abundances from this measurement. However, when the lines were severely blended, or affected by fine or hyperfine structure (FS or HFS), a synthetic spectrum was computed over several Å and compared to the observed one. A complete list of the atomic lines used, with their excitation potential and oscillator strength and the measured equivalent widths can be found in the Appendix[1]. Although the abundance of the elements have been computed line by line, as an illustration of the correct choice of the parameters of the model and of the precision of the abundance determination, a typical curve of growth obtained with the Fe1 line is given in Fig. 2.

3.4. Molecular bands analysis

In cool stars, the light elements (carbon, nitrogen and oxygen) are partly locked in molecules (CN, CO, C_2), Spectrum synthesis calculations were carried out to derive the carbon and nitrogen abundances from C2 and CN features. Moreover, since the [O I]λ6300 Å line and the Li Iλ6707.8 Å are blended by CN bands, the abundance of these two elements was also deduced from comparison to synthetic spectra.

As in Paper II, the spectrum synthesis code use is that of Barbuy (1981), descibed in Cayrel et al. (1991). The details on the molecular data, in the wavelength range treated here, are given in Milone et al. (1992). The regions and bandheads used for the abundance derivation are given here:

Oxygen abundances were derived using the forbidden [O I]λ6300.311 Å line, taking into account the C and N abundances found for each star.

Carbon: the C_2(0,0)5165.24 Å and C_2(0,1)5635.50 Å bandheads of the Swan ($A^3\Pi_g$ - $X^3\Pi_u$) system were used to derive the carbon abundances. The C_2(0,1) feature is weak in all the stars for which it is available. The C_2(0,0) feature is stronger and, although blended with atomic lines and MgH, is more reliable. The values tabulated in Table 4 are thus the ones derived from the C_2(0,0) feature. In most stars, where both features were measurable, the two features give the same abundance.

Nitrogen abundances were derived from the CN red system ($A^2\Pi$ - $X^2\Sigma$) bandhead (6,2)λ6478.48 Å.

Lithium abundances were derived from the 6707.8 Å line, taking into account the nearby atomic lines (and gf values) following Lambert et al. (1993) and the CN features.

3.5. Abundance uncertainties

For a extended discussion of the expected intrinsic errors expected for such an analysis, one should turn to the Sect. 4.1 and Table 4 in Paper I and Sect. 4.2.

In short, for all supergiants, we concluded that the typical errors in the determination of the effective parameters of the stars are the main source of star-to-star abundance uncertainty and are likely to produce overall shifts in the absolute iron abundance of $\leq$ 0.15 dex, and errors on the abundance ratios around 0.10 (and seldom up to 0.2 dex where low excitation potential lines are concerned).

4. Comparison NGC 330 stars versus field stars

Tables 4 gives the detailed abundances derived for each of the six program stars.

The sample of 6 K type supergiants in the field of the SMC studied in Paper I provides a perfect reference to investigate the difference between the chemical composition of stars with similar ages, in NGC 330 and in the surrounding field:

[1] available via anonymous ftp copy at the CDS

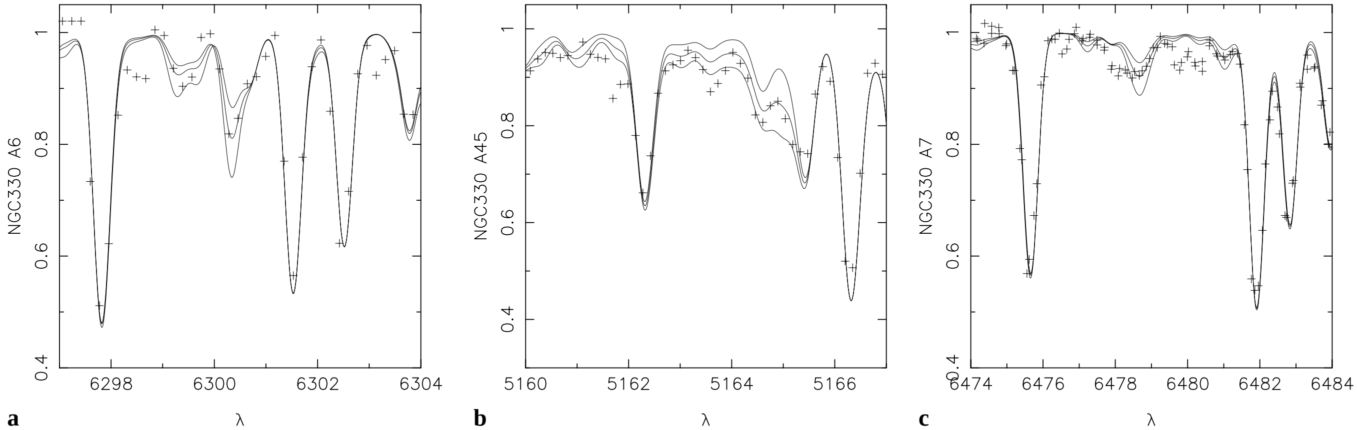

Fig. 3a–c. Examples of the fitting of the [OI] line and molecular bands. **a** Forbidden [OI]λ6300 Å in the star NGC 330 A6. The solids lines showed here are for abundances of oxygen of [O/Fe] = +0.05, −0.15 and −0.35 dex **b** C_2(0,0)5165.24 Å bandhead of NGC 330 A45.The solids lines showed here are for abundances of carbon of [C/Fe] = −0.10, −0.20 and −0.40 dex. **c** CN(6,2)λ6478.48 Å bandhead of NGC 330 A7. The solids lines showed here are for abundances of nitrogen of [N/Fe] = +0.10, −0.10 and −0.30 dex.

– The stars are physically very similar (temperature, gravity) so that the possible errors in the model atmospheres/ physical parameters of the lines cancel out when one considers the differential abundances of the stars.
– The method to determine the effective parameters of the stars were the same in both samples so that possible systematical errors also cancel out.

4.1. Metallicity

The mean iron deficiency and standard deviation of the two samples are respectively $\overline{[Fe/H]}$ =-0.82$\pm$0.10 dex and $\overline{[Fe/H]}$ =-0.69 $\pm$ 0.11 dex. The two histograms on Fig. 4a show that there is a small but sytematic shift between the distribution of [Fe/H] in the SMC field and NGC 330. However, this difference is small ($\Delta([Fe/H])$ =-0.13 dex), much smaller than what was found in earlier works.

Fig. 4b is a comparison of the NGC 330 sample against the total number of F to K type supergiants studied to date in the SMC (compilation by Luck et al. 1998, including cepheid variable supergiants). The overall metallicity distribution compiled by Luck et al. 1998 is very similar to the one found in Paper I, given the different sizes of the samples. Let us note that the outlier, most metal poor star in the Luck et al. 1998 compilation is a cepheid from Luck and Lambert 1992, and its abundance is subject to caution: for the three cepheids that they had in common with Luck and Lambert 1992, Luck et al. 1998 found abundances differences as great as 0.4 dex.

There again, the small but systematic shift of NGC 330 towards the metal-poor end is visible.

4.2. Abundance ratio pecularities

Fig. 5 displays the mean [X/Fe] ratios (abundance relative to iron) versus the atomic number of the element for the field (filled circles) and the cluster (open circles) samples. The "error bar" plotted here is the sample's 1σ dispersion around the mean. *The similarity of the abundance pattern is striking: for most elements, the mean abundance of the two samples differ by less or of the order of the σ deviation.* This overall very close similarity of abundance pattern argues in favour of a formation of the cluster from matter which has experienced the same chemical history as the coeval field component of the SMC.

On the other hand, the abundance ratios of a few elements differ slighlty from cluster to field. These are namely oxygen, and some of the heaviest neutron capture elements (Ba, Nd).

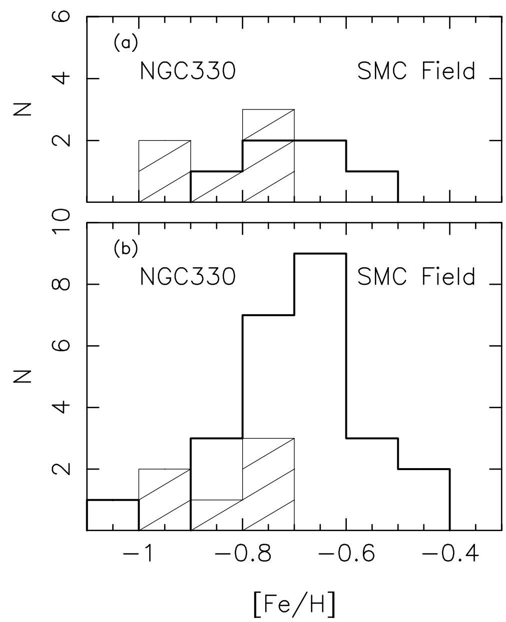

Fig. 4a and b. [Fe/H] histograms for the supergiants in the field of the SMC (solid thick line) and in NGC 330 (dashed area). In panel **a**, the field data are from Paper I, whereas in panel **b**, the field data are all the known F to K type supergiants of the SMC (compilation by Luck et al. 1998, including cepheids)

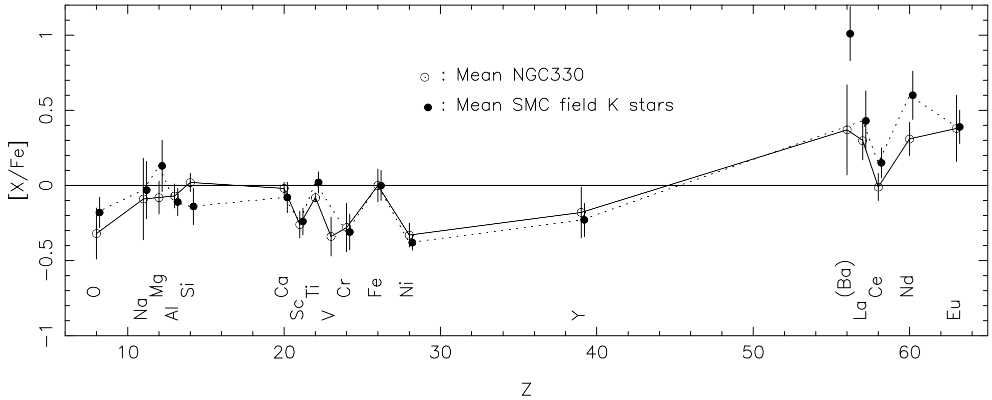

Fig. 5. [X/Fe] ratios versus atomic number (Z) for the mean of the six K supergiants in the field of the SMC (filled symbols, solid line) and the six cool supergiant of our sample in NGC 330 (open symbols, dashed line). The "error bar" is the sample's standard deviation (1σ) around the mean value for each element

Table 4. Abundances for the six cool supergiant stars

Star	A3			A6			A7			A14			A45			B40		
	4800, 0.5, 3.			4250, 0.0, 3.			4000, −0.3, 3.			4100, −0.4, 3.			4400, −0.1, 2.3			4300, 0.2, 3.		
(FeI+FeII)/2	−0.72			−0.91			−0.76			−0.84			−0.98			−0.72		
log ϵ(Li)	<0.70		1	−0.10		1	−0.15		1	0.20		1	0.30		1	0.10		1
C[1]	−0.92			−1.01			−1.16			−1.24			−1.18					
N[2]				−0.71			−0.76			−0.84			−0.83			−0.72		
O I	−1.27		1	−1.06		1	−1.16		1	−1.24		1	−1.33		1	−0.82		1
Na I	−0.99	0.21	3	−0.93	0.04	3	−0.33	0.05	4	−1.02	0.02	3	−1.16	0.14	3	−1.02	0.04	2
Mg I	−0.85	0.01	2	−1.00	0.28	2	−0.77	0.08	2	−0.79	0.08	2	−1.21	0.23	2			
Al I				−0.89		1	−0.85	0.16	2	−1.00	0.09	2	−0.98	0.25	2	−0.84	0.27	2
Si I	−0.80	0.14	7	−0.86	0.14	8	−0.71	0.24	8	−0.76	0.19	8	−0.95	0.14	8	−0.73	0.20	8
Ca I	−0.69	0.26	16	−0.90	0.23	13	−0.86	0.20	9	−0.87	0.19	11	−1.01	0.27	15	−0.73	0.17	11
Sc II	−0.93	0.17	6	−1.15	0.18	7	−0.96	0.34	5	−1.11	0.22	6	−1.42	0.19	6	−0.95	0.07	2
V I	−1.13	0.24	7	−1.14	0.21	12	−1.15	0.10	9	−1.34	0.16	10	−1.13	0.21	12	−1.08	0.16	12
Ti I	−0.78	0.25	35	−0.95	0.23	43	−0.89	0.17	22	−0.94	0.28	35	−1.03	0.25	45	−0.81	0.20	23
Cr I	−0.99	0.47	6	−0.96	0.42	9	−1.23	0.40	4	−0.98	0.46	5	−1.30	0.22	6	−1.12	0.31	5
Fe I	−0.75	0.20	118	−0.90	0.27	116	−0.79	0.17	63	−0.85	0.23	94	−1.03	0.24	118	−0.74	0.17	63
Fe II	−0.70	0.19	10	−0.92	0.19	13	−0.73	0.17	10	−0.83	0.25	10	−0.94	0.22	17	−0.70	0.10	10
Co I	−1.12	0.45	2	−1.13	0.41	6	−1.60	0.30	2	−0.72	0.49	3	−1.20	0.23	3	−1.21	0.42	3
Ni I	−1.09	0.25	11	−1.10	0.19	12	−1.13	0.18	9	−1.23	0.20	10	−1.29	0.20	8	−1.09	0.09	6
Y II	−0.99	0.21	2	−0.83	0.01	2	−1.00	0.24	3	−1.19	0.23	3	−1.11	0.08	2			
Ba II	−0.45		1	−0.52	0.36	3	−0.50	0.14	2	−0.52		1	−0.94	0.27	3	0.20	0.00	2
La II	−0.56	0.20	2	−0.51	0.08	2	−0.55	0.07	2	−0.57		1	−0.72	0.11	2	−0.22	0.11	2
Ce II	−0.78	0.10	4	−0.81	0.06	4	−0.76	0.05	4	−0.94	0.09	4	−1.09	0.17	4	−0.63		1
Nd II	−0.58	0.09	2	−0.47	0.06	4	−0.41	0.08	4	−0.55	0.11	4	−0.66	0.14	4			
Eu II	−0.51		1	−0.43		1	−0.35		1	−0.71		1	−0.67		1	0.04		1

Notes: The abundances are given relative to the Sun, i.e. [X/H]. On the contrary, the lithium abundance is in the scale log ϵ(H)=12.
1: from C_2 molecular bands
2: from CN molecular bands

In the following paragraphs, we review the different groups of elements and their peculiarities.

4.2.1. Lithium, carbon, nitrogen

In evolved stars such as red supergiants, the abundances of these elements are affected by events such as first dredge-up. During such phases, deep convective movement drege-up towards the surface the fresh products of the CNO cycle that operated while the star was on the MS. Lithium abundances are also altered in the process, since the newly dredged-up gas comes from hotter layers of the stars where lithium is heavily distroyed. Lithium is thus strongly diluted in the process.

As discussed in details in Paper II, the cool field supergiants in the SMC display evidences of this first dredge-up deep mixing, showing enhanced [N/Fe] and low [C/Fe] ratios, and low lithium content. The stars in NGC 330 also show the same feature, although there is an indication that these supergiants might have experienced slightly less mixing than their field couterparts. Fig. 6 shows that indeed, the C/N ratios of the cluster stars are smaller in average than those in the field stars. Lithium is also detected in the five cooler stars, with abundances log ϵ(Li)

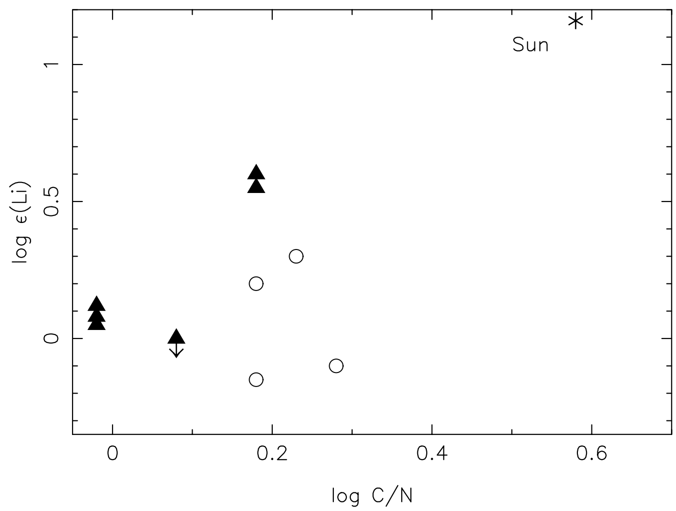

Fig. 6. Lithium abundance log ϵ(Li) versus C/N ratios for the cool supergiants in the field from Paper II (*filled triangles*) and NGC 330 (*open circles*).

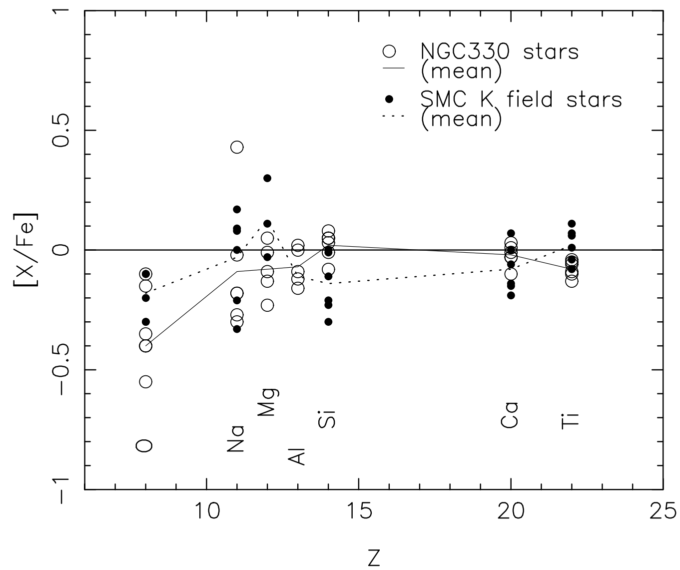

Fig. 7. Detailed abundance patterns of the α elements for the six supergiants in the field of the SMC from Paper I (*filled circles*) and the present six NGC 330 stars (*open circles*).

ranging from −0.15 to +0.3 dex. In the star A3, with a temperature of 4800 K, the line is not visible, which is expected if the log ϵ(Li)≃0.0 dex (the expected equivalent width would be only W=2.mÅ!). We could therefore only estimate an upper limit of log ϵ(Li)<0.7 dex, assuming that we would have detected the line if it had been more than 10mÅ. As can be seen in Fig. 6, the lithium abundances found here are similar to what is found in the field stars, however somewhat skewed towards the lower values.

Let us finally note that the [C+N/Fe] ratio, tracing the abundance of C and N, but mostly *independent* of mixing effects, is similar in the cluster and the field stars (mean and σ deviation of −0.17±0.10 and −0.15±0.08 dex respectively in each sample), at clear variance to what is observed in the H II regions of the Magellanic Clouds, where carbon is measured to be strongly depleted (see discussion in Paper II).

4.2.2. α-elements

The so-called α-elements are also, in the mean, very similar, as can be seen from Fig. 7. The [Ti/Fe] and [Ca/Fe] abundances are solar in both the cluster and field stars. [Mg/Fe] also appears to be around solar in the cluster (but could however be slightly over-solar in the field).

However, the behaviour of the oxygen abundance is somewhat more complicated. In the field of the SMC (cf. discussion Paper II, Sect. 5.1), the oxygen abundances seem to be following very closely that of the iron (ie. [O/Fe] constant). However, in the cluster, the [O/Fe] ratio is somewhat more dispersed, ranging from −0.55 to −0.1 dex (a factor 3 difference), and resulting in a slightly lower mean value ($\overline{[O/Fe]} = -0.32 \pm 0.17$ compared to −0.18±0.10 dex in the field where the values range from −0.10 to −0.30 dex). This feature needs to be confirmed, since the forbiden [OI]λ6300 Å line is not a very strong feature (cf. Fig. 3), and the resolution of the CASPEC spectra is just sufficient to disantangle the smaller Sc II line blending the oxygen line redwards (the situation in Paper II was better since the resolution of the EMMI spectra used was higher). This feature, if confirmed, would be similar to the dispersion of oxygen content found among stars within several Galactic globular clusters (see for example the recent rewiew by Kraft 1998).

We note however that the cluster stars whith [O/Fe] ratios differing the most from the field stars value are those with very low [O/Fe], excluding the possibility of self-enrichement of the cluster as a cause for the large scatter: early explosion of massive SN II contaminating the gas in which the cluster form would produce high [O/Fe] outliers.

4.2.3. Iron group elements

The elements of the iron group (Sc, Cr, Ni) abundances (relative to iron) are all extremely similar in NGC 330 and in the field. This feature is expected, regardless of the cluster formation process involved.

Let us note, however, a peculiarity (already noted in Paper I): the nickel to iron ratios are sub-solar in all the twelve stars, whether in the cluster or the field. This effect ([Ni/Fe] = −0.35 dex) is too large to be explained by abundance determination errors, since the stars effective parameters have little influence on the [Ni/Fe] ratio. Also, the [Ni/Fe] ratio do not correlate with any of the parameters of the stars, nor with any of the other element ratios: it is essentially constant for all twelve stars. On the other hand, Welty et al. 1997 also found that Nickel was over deficient (relative to Zn) in the ISM of the SMC (provided that the locking of Ni in grains is similar to what is observed in the Galactic ISM). If this overdeficiency of the nickel relative to iron was to be real in the SMC, it would indeed be very difficult to explain within the standard nucleosynthesis and chemical

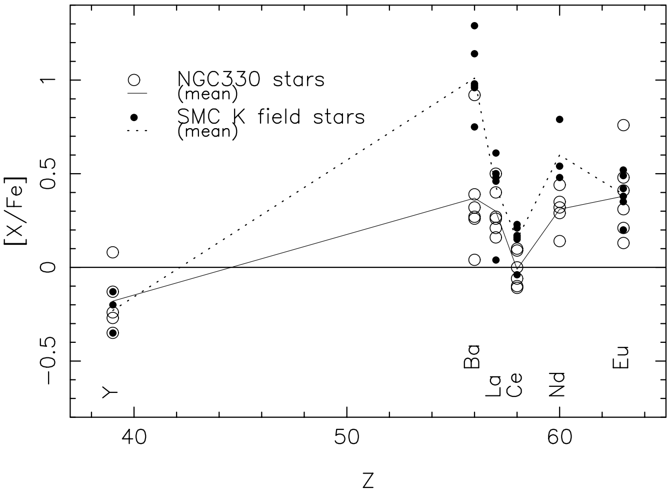

Fig. 8. Detailed abundance patterns of the neutron-capture elements for the six supergiants in the field of the SMC from Paper I (*filled circles es*) and the present six NGC 330 stars (*open circles*).

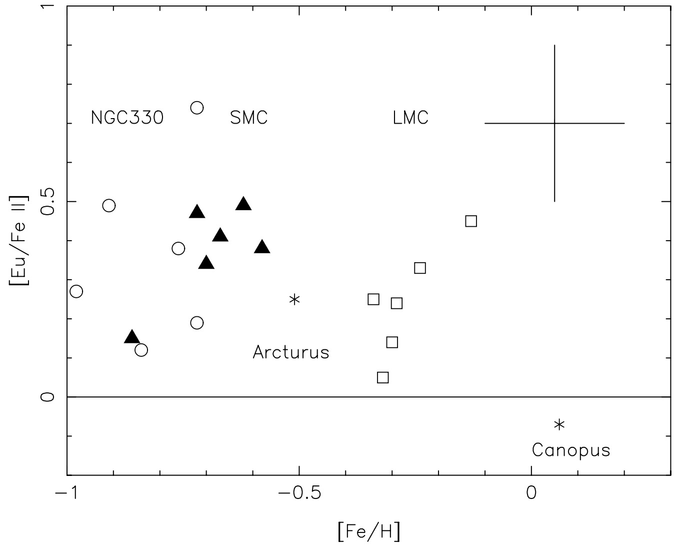

Fig. 9. [Eu_{II}/Fe_{II}] versus [Fe_{II}/H] for supergiants in the field of the LMC from Hill et al.. 1995 (*open squares*), the field of the SMC from Paper I (*filled triangles*) and NGC 330 (*open circles*)

evolution framework: nickel is thought to be produced in the same mass-range and same astrophysical sites, namely, mostly by SN I.

4.2.4. Neutron-capture elements

The heavier component of the neutron-capture elements (Z≥56) has been long been observed to be enhanced in both Magellanic Clouds (Spite et al. 1986, Russell&Bessell 1989, Luck&Lambert 1992), the effect being greater in the SMC than in the LMC. On the other hand, lower mass neutron-capture elements such as Y or Zr were not enhanced. This effect is very unique of the Magellanic Clouds, and is not observed in any Galactic supergiants. Fig. 9 illustrates this feature.

The high abundances of elements such as Ba, Ce, Ne and Eu found here are in agreement with this general finding, for all stars studied. This can be seen on Fig. 8 where the heavy neutron-capture elements abundances (relative to iron) are plotted as a function of the atomic mass of the element, for the NGC 330 supergiants and the field sample from Paper I. Again, the somewhat lighter element Y is not enhanced. However, one might note that, while europium is very similar in both the field and the cluster supergiants, there is a sytematic tendency of barium, lanthanium, cerium and neodynium to be less enhanced in the cluster than it is in the field.

We would like to recall that Eu is thought to be an almost pure product of the r-process, while Ba is thought to be almost purely issued from s-process, and La, Ce, Nd are produced in significant fraction by both processes. Therefore, europium is thought to be produced in SN II, whereas barium is observed to be produced efficiently in AGB stars. The incontrovertible Eu overabundance in the Magellanic Clouds is very difficult to reconcile with the picture that one could deduce from the pattern of other elements: α-elements are also massively produced in SN II, and they show *no evidence of enhancement* in the Magellanic Clouds supergiants (see discussion on oxygen in Paper II).

5. Conclusions

Taking advantage of our previous high resolution analysis of a sample of in the SMC field type K supergiants (Paper I and II), we analyse 6 cool supergiants in NGC 330, in order to compare, in an homogeneous way, the metallicity and abundance ratios of various elements in NGC 330 and in the field of the SMC.

The main results are that the deficiency of NGC 330 is found to be of [Fe/H] = -0.82 ± 0.11 dex (mean and rms for 6 stars) whereas the field stars had a [Fe/H] = -0.69 ± 0.10 dex (mean and rms for 6 stars). A slight difference may exist between the field and the cluster stars, but this difference is small. Moreover, the similarity of the abundance pattern is striking: for most elements, the mean abundance of the cluster and field samples differ by less or of the order of the 1σ deviation. This overall very close similarity of abundance pattern argues in favour of a formation of the cluster from gas which has experienced the same chemical history than the bulk of the SMC. More specifically, there is no room for a self-enrichement of the cluster (through the early explosion of massive SN II).

A few peculiarities of the cluster with respect to the coeval SMC field stars were also noted:

• Oxygen's star to star scatter is larger in the cluster.

• lithium is detected in five stars and is low, indicating that the stars underwent dilution (mean value and rms for the 5 stars: $\log\epsilon(Li)\simeq 0.1\pm0.2$ dex), but the mixing indicator C/N ratio (the lower the ratio the higher the mixing) is somewhat larger in the cluster, indicating a less efficient mixing of CNO burning cycle products.

• while Eu is enhanced (relative to iron) by the same factor, other heavy neutron-capture elements (which can be produced by both *r*- and *s*- processes) are less enhanced in the cluster stars.

Finally, we would like to stress once more the very poor understanding that we have of the behaviour of the heaviest neutron-capture elements in the Magellanic Clouds. As discussed in Sect. 4.2.4 This issue will probably not make any significant progress until abundance ratios are measured in older population of stars in the Magellanic Clouds, so as to trace the *evolution* of the various elements with time. This in turn, will have to wait for 8m class telescopes operating with high spectral resolution spectrographs to become available in the Southern Hemisphere.

Acknowledgements. We thank M. Bessell for very useful discussion about the color-temperature relation, and the communication of $(V-K)$ colours for the stars in our sample.

We acknowledge E. Maurice for kindly lending us the CCD data for the BVRI photometry of NGC 330.

We also thank B. Plez for communicating his most recent yet unpublished models.

References

Alcaino G., Alvarado F., 1988, AJ 95, 1724
Barbuy B., 1981, A&A 101, 365
Bessell M., 1991, In: Haynes R., Milne D. (eds.) The Magellanic Clouds. IAU symp. 147, Kluwer, Dordrecht, p. 273
Bessell M., 1995, private communication
Bessell M., Castelli F., Plez B., 1998, A&A 333, 231
Caloi V., Cassatella A., Castellani V., Walker A., 1993, A&A 271, 109
Carney B.W., Janes K.A., Flower P.J., 1985, AJ 90, 1196
Cayrel R., Jugaky J., 1963, Ann. d'Astrophys. 26, 495
Cayrel R., Perrin M.-N., Barbuy B., Buser R., 1991, A&A 247, 108
Grebel E., Richtler T., 1992, A&A 253, 359
Hilker M., Richtler T., Gieren W., 1995, A&A 294, 648
Hill V., Andrievsky S., Spite M., 1995, A&A 293, 347
Hill V., 1997, A&A 324, 435 (Paper I)
Hill V., Barbuy B., Spite M., 1997, A&A 323, 461 (Paper II)
Jasniewicz G., Thévenin F., 1994, A&A 282, 717
Kraft R.P., 1998, In: Spite M. (ed.) Galaxy evolution: Connecting the Distant Universe with the Local Fossil Record. Conf. held in Paris sept. 98, Kluwer, Dordrecht, (in press)
Lambert D.L., Smith V., Heath J., 1993, PASP 105, 568
Luck R.E., Moffett T., Barnes T., Gieren W., 1998, AJ 115, 605
Luck E., Lambert D., 1992, ApJS 79 303
Milone A., Barbuy B., Spite M., Spite F., 1992, A&A 261, 551
Meliani M.T., Barbuy B., Perrin M.-N., 1995, A&A 300, 349
Plez B., Brett J.M., Nordlund A., 1992, A&A 256, 551
Plez B., 1995 and 1997, private communication
Robertson J.W., 1974, A&AS, 15, 261
Russell S., Bessell M., 1989, ApJS 70, 865
Russell S., Dopita M.A., 1990, ApJS 74, 93
Russell S., Dopita M.A., 1992, ApJ 384, 508
Spite M., Cayrel R., François P., Richtler T., Spite F., 1986, A&A 168, 197
Spite M., 1990, In: Baade D., Grøsbol P.J. (eds.) 2nd ESO/ST-ECF Data Analysis Workshop. ESO Conference and Workshop Proceedings No. 34, p. 125
Spite F., Richtler T., Spite M., 1991, A&A 252, 557
Vigneau J., Azzopardi M., 1982, A&AS 50, 119
Welty D., Lauroesch J., Blades J., Hobbs L., York D., 1997, ApJ 489, 672